land

MDPI

Article

Past and Future Land Use/Land Cover Changes in the Ethiopian Fincha Sub-Basin

Motuma Shiferaw Regasa and Michael Nones *

Institute of Geophysics, Polish Academy of Science, 01-452 Warsaw, Poland
* Correspondence: mnones@igf.edu.pl

Abstract: The increasing human pressure on African regions is recognizable when looking at Land Use Land Cover (LULC) change maps, generally derived from satellite imagery. Using the Ethiopian Fincha watershed as a case study, the present work focuses on (i) identifying historical LULC change in the period 1989–2019; (ii) estimating LULC in the next thirty years, combining Geographical Information Systems (GIS) with Land Change Modelling (LCM). Landsat 5/8 images were combined with field evidence to map LULC in three reference years (1989, 2004, 2019), while the Multi-Layer Markov Chain (MPL-MC) model of LCM was applied to forecast LULC in 2030, 2040, and 2050. The watershed was classified into six classes: waterbody, grass/swamp, built-up, agriculture; forest; and shrub. The results have shown that, in the past 30 years, the Fincha watershed experienced a reduction in forest and shrubs of about −40% and −13%, respectively, mainly due to ever-increasing agricultural activities, and such a trend is also expected in the future. In fact, for the period 2019–2050, LCM simulated a significant decrease in both forest and shrubs (around −70% and −20%, respectively), in favor of more areas covered by grass (19%) and built-up (20%). It is worth noting that a decrease in natural forests can drive an increase in soil erosion, fostering siltation in the water reservoirs located in the sub-basin. The study pointed out the urgency of taking actions in the sub-basin to counteract such changes, which can eventually lead to a less sustainable environment.

Keywords: Ethiopia; Fincha river; land use land cover; land change modeler; multi-layer Markov chain

Citation: Regasa, M.S.; Nones, M. Past and Future Land Use/Land Cover Changes in the Ethiopian Fincha Sub-Basin. *Land* **2022**, *11*, 1239. https://doi.org/10.3390/land11081239

Academic Editor: Le Yu

Received: 13 July 2022
Accepted: 3 August 2022
Published: 4 August 2022

1. Introduction

Land use is defined as how land is utilized by human beings and their habitats, usually with an accent on the practical role of land for economic activities, whereas land cover is a physical characteristic of the Earth's surface or attributes of a part of the Earth's land surface and immediate subsurface, including biota, soil, topography, surface and groundwater, and human structures [1–4]. As it is strictly connected with representing the hydrological cycle [5,6], land use and land cover (LULC) change has been one of the most widely used methods to understand past land uses, types of changes estimated, the forces behind such changes, and the perceptible transformations of the Earth's surface [1]. LULC changes could involve critical issues such as biodiversity degradation and negative impact on human life [7,8]. The study of LULC change has attracted growing interest in recent years and is a complex issue that involves physical, environmental, and socioeconomic facts. According to Lambin et al. [9], the modeling of land cover processes can answer questions such as (i) which are the main environmental and cultural variables that contribute most to the observed changes, and why? (ii) within a geographical region, which locations can be affected by land cover changes, where and at what rate does land cover change, and when?

Prediction using time series data is important for the future management plan of LULC, and it is frequently employed as a diverse appropriateness measure as a proxy of human influence on land change processes [4,10]. Analysis of the historical trends of LULC is paramount in modeling future LULC, as past information generally represents a good proxy of human influence on land processes [10,11]. To adequately predict future scenarios,

models should be calibrated and validated, and various techniques are available in the literature. Geometric rectifying, supervised and unsupervised classification methods, post-classification method, GIS spatial analysis, Markov chain analysis, the ERDAS IMAGINE model, and the Land Change Modeler (LCM) were used to analyze historical LULC change and predict future changes [12–15].

The Land Change Modeler is a model used to evaluate the changing trend from one land use category to another and has been found to provide high spatial and temporal resolution with a reduced computational effort [16,17]. The integrated CA-Markov model is a robust technique in terms of quantity estimation as well as spatial and temporal dynamic modeling of LULC because remote sensing data and GIS can be proficiently incorporated. The integrated CA-Markov model can translate the results of the Markov chain model to spatially explicit results [18]. The Markov model has been widely adopted in ecological studies, and its applicability in LULC change modeling is promising because of its ability to quantify not only the states of conversion between land-use types but also the relative rate of conversion [19,20]. The CA-Markov model is a watershed-scale model that combines the link between LULC and drivers to physically model spatial changes [21] and anticipate geographical and temporal patterns with high simulation accuracy and is therefore well suited to long-term forecasting. Understanding the forms and the driving forces of LULC change is essential for providing rational and specific planning of viable land management [22]. Quantitative studies of the relationship between driving forces [23] and LULC are primarily undertaken using mathematical approaches and statistical methods such as principal component analyses or traditional correlation analysis [24]. System dynamics models, prediction models, Markov models, regression statistical models, and other models are also largely adopted in evaluating and predicting LULC changes at the watershed scale.

Few studies of LULC change provide a combined assessment of the driving forces and consequences of such variations, particularly in developing countries such as Bangladesh [25,26] and India [27] and in Africa [28,29]. Recent research focused on sub-Saharan Africa, showing a decrease in land covered by the natural environment, mostly due to human activities such as population growth, economic development, and globalization [30–32]. However, only recently have scholars been looking to explicitly connect such variations with nature-related aspects such as the loss of ecosystem services [33–36], eventually providing policy implications and management strategies. Looking at past and predicted LULC changes in a small sub-basin, the present study will contribute to the discussion, providing some evidence on LULC trends that are typical of the sub-Saharan areas.

Indeed, in this region, the dynamics of LULC intensities and rates are changing and highly associated with overexploitation of natural resources, while the process is governed by climate (long dry periods followed by heavy precipitation), soil characteristics (thin layer of topsoil, silty texture, or low organic matter content), vegetation (barren land), topography (steep-slope), and natural hazards (forest fire, landslides) [17,37]. During the last decades, the human pressure has increased significantly, therefore the process has been accelerated considerably. In Ethiopia, LULC changes are generally persistent events where agricultural activities and settlements are dominant in the rural landscape [38–41]. For example, Tadese et al. [4] reported that agricultural fields and settlements increased by around 17% and 3%, respectively, from 1987 to 2017, while forested land decreased by 78%.

Focusing on the Fincha River sub-basin in Ethiopia, this research aims to: (i) understand the historical LULC changes over the past three decades (1989–2019); (ii) predict possible LULC patterns in the future three decades (2030–2050). The objectives of the paper will be tackled by combining satellite imagery (Landsat dataset) and modeling (LCM), using field evidence such as photos and information from local farmers to support the study. The study area and the methods used will be described in Section 2, while the results are presented and discussed in Section 3. In Section 4, the results are then discussed in light of actual policies on land management, showing the current limitations and possible future directions. The main outcomes of the study and its limitations are summarized in Section 5.

2. Materials and Methods

2.1. Study Area

The Fincha sub-basin is located in Ethiopia, Oromiyaa regional state, Horroo Guduruu Wallaggaa, in the Upper Blue Nile basin (UBNB), between latitudes 9°9′53″ N to 10°1′00″ N and longitudes 37°00′25″ E to 37°33′17″ E, at around 300 km from Addis Ababa (Figure 1b). The watershed is bounded to the south by the Great Gibe River basin, on the north by the Abbay River basin, on the west by the Didessa sub-basin, and on the east by the Guder sub-basin. The overall study area covers about 3781 km^2, containing three sub-basins, namely the Fincha, Amerti, and Neshe. The altitude of this sub-basin spans from around 970 m asl in the northern lowlands to more than 3200 m asl in the southern part (Figure 1c). A detailed description of the study area is reported in the recent work of Kenea et al. [7].

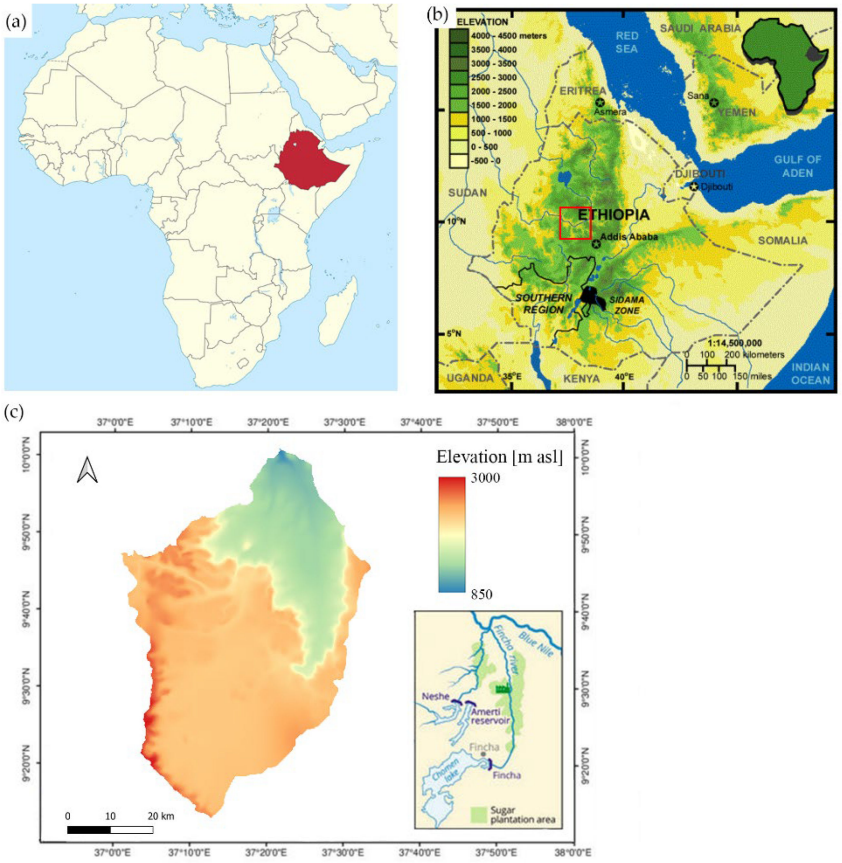

Figure 1. (**a**) Map of Africa with Ethiopia highlighted; (**b**) map of Ethiopia showing ground elevation [m as]; (**c**) Digital Elevation Model of the Fincha sub-basin and location of the main reservoirs in the Fincha sub-basin. The map was adapted from [7].

Four main seasons characterize the region: Summer, from June to August, with heavy rainfalls; Autumn from September to November (called harvest season); Winter, from December to February (the dry season with frost in the morning, especially in January); Spring, from March to May (occasional showers and the hottest season). The annual rainfall in the study area ranges between 1367 and 1842 mm with the minimum rainfall occurring in the northern lowlands and maximum rainfall greater than 1500 mm in the southern and western highlands. June to September is the main rainy season of the catchment, with an average of 1604 mm and maximum rainfall between July and August.

Natural resources, such as the Fincha, Amarti, and Nashee lakes (see Figure 1c), contribute to the national economy by generating hydroelectric power but are also used for irrigating large fields devoted to sugar cane. The area is of interest for national and

international hydro-politics due to its downstream connection to the Nile basin and its intense agriculture.

2.2. Dataset

The study was performed using freely available satellite imagery and a Digital Elevation Model (DEM). The latter, having a resolution of 30 m and referring to 2019, was acquired from the GIS and Remote Sensing Department, Ministry of Water, Irrigation and Energy of Ethiopia [42].

Landsat-5 TM (L5, for the years 1989 and 2004) and Landsat-8 OLI-TIRS (L8, for the year 2019) data were downloaded from the United States Geological Survey (USGS) website (earthexplorer.usgs.gov). As the Landsat-5 mission started in March 1984, it was not possible to acquire the images every 10 years, so the first reference year was set to 1989. The images referred to January, when there is a clear sky corresponding to the dry season, and were atmospherically corrected via QGIS (qgis.org). To cover the whole watershed area, a composite of Landsat images from different paths/rows was created, ensuring that the images refer to the same season (Table 1).

Table 1. Details of the Landsat images that were analyzed in the study.

Satellite	Year	Acquisition Date	Path/Row	Spatial Resolution
Landsat 5 TM	1989	January 4	169/53, 169/54	30 m
		January 11	170/53	30 m
Landsat 5 TM	2004	January 11	170/53	30 m
		January 15	169/53, 169/54	30 m
Landsat 8 OIL	2019	January 14	170/53	30 m
		January 23	169/53, 169/54	30 m

Field surveys have been conducted to assist the LULC classification of the satellite images. In addition, key informant interviews (KII) and focal group discussions were performed to obtain socio-economic support data, as this is paramount to understanding how locals interact with the environment [39–45]. KII were conducted with elders, as they have known the area for at least 30 years and have good knowledge of past LULC changes. Focal Group Discussions (FGD) were conducted with experts from zonal and district offices of agriculture; natural resources management; environment and climatic change; land use administration, and with local people's representatives. Ground truth data were collected using GPS and digital cameras to evaluate the current LULC.

Open-ended questions about LULC's significant changes in the study area, the connection between the biophysical environment, institution, socioeconomic activity, and demography were utilized during both KII and FGD. To learn more from a management point of view, assess the efforts made towards resource management, and identify obstacles, discussions on the practices and regulations that affect land management and policies in the area were held. The topic of land degradation and the most urgent problems that need solutions were also covered. The major goals of the discussion and interviews were to gather enough information on the historical and present trends of LULC changes, identify their fundamental causes, and assess their effects on regional socio-economic life and the environment. In detail, farmers were asked to describe the areas of the landscape that have altered and to recognize the reasons behind those changes. Moreover, they were questioned on the effects of the modifications to their way of life, their surroundings, and their working environment. In addition, farmers were asked to describe how their socioeconomic activity affects the change in land usage.

Based on a checklist created in advance to assess the situation in the watershed, field observations were conducted, and images of significant sites were obtained.

2.3. Land Use Land Cover Classification of Historical Data

To map LULC, satellite images should be classified, assigning predefined LULC classes to some pixels. As pointed out by Jemberie et al. [44], this phase could be affected by various factors such as classification methods, algorithms, collecting of training sites, and the quality (correctness) of the classification should be assessed via field evidence [46,47].

The study was performed by classifying three reference years (1989, 2004, and 2019) and considering six LULC classes. The selection of these classes was performed based on past studies [7], field evidence, and information coming from local farmers and experts, as well as the personal considerations of the authors. Based on this, the Fincha sub-basin was classified into six classes, namely waterbody, built-up (urban and rural settlement), agriculture, forest (dense forest and sparse/desert forest), grass, and swamps (Table 2).

Table 2. Land Use Land Cover classes and their description.

LULC Classes	Description
Waterbody	area completely covered by waters such as lakes, rivers, and ponds
Built-up	area covered by urban and rural settlements, roads, industries, infrastructures
Agriculture	area covered by annual and perennial crops
Forest	area covered by evergreen forest
Shrub	area with trees that are not evergreen during the dry season
Grass/Swamp	area covered with grasses used for grazing, and sugarcane plantations

In the process of classification, it is difficult to differentiate some LULC classes' spectral properties from other classes. For instance, sugar cane, currently planted for the Fincha sugar factory, and grass; urban and rural settlements, roads, industries, and infrastructures have the same properties. This happens because the spectral properties of some LULC classes appear identical to others. To simplify the complexity and reduce the number of LULC classes, some related LULC classes were merged to form one class. For example, urban and rural settlements, roads, industries, and infrastructures were aggregated as built-up, while grass, swamps, and land that is covered by sugar cane, were commonly named grass/swamp.

Following ample literature on this topic e.g., [46–50], the maximum likelihood supervised classification method was applied via ArcGIS by creating training sites. For the L8 image of 2019, such training sites were defined using 100 ground truth points, while, for the two older L5 images, training signature sites were defined via unsupervised classification, ancillary data (Google Earth and Copernicus data), and KII information and literature data [7]. To improve image quality, quality assessments were used by taking a total of 50 ground truth points (20 agriculture, 5 waterbody, 5 built-up, 10 forest, 5 shrub, and 5 grass/swamps). The points were uniformly distributed across the watershed to guarantee a proper classification.

To quantitatively assess the accuracy, statistical methods such as overall accuracy and kappa value were applied. Based on this, random sampling data were prepared to check the overall accuracy *OA* and to determine the kappa coefficient *K*. Comparing the total corrected samples *TCS* and the total samples *TS*, *OA* provides an idea of how many sites are correctly classified (Equation (1)), and ranges from 0 (corrected samples) to 1 (very accurate classification).

$$OA = \frac{TCS}{TS} \quad (1)$$

The kappa coefficient *K* (Equation (2)) is generated from a statistical test and describes the accuracy of a classification compared to a random classification [51,52]. Its value varies between 0 and 1, where 0 indicates a total accidental classification, while 1 indicates a very

accurate classification. According to Gidey et al. [53], good classifications have $K > 0.8$, while bad classifications have $K < 0.4$.

$$K = \frac{[TS * TCS - \sum(ColumnTotal * RowTotal)]}{TS^2 - \sum(ColumnTotal * RowTotal)} \quad (2)$$

where the matrix columns indicate the correspondence between ground truth data and the pixel location, while the matrix rows indicate to which class the is pixel assigned.

2.4. Prediction of Future LULC and Associated Driving Forces

To manage natural resources (biodiversity) influences, and to analyze and forecast spatial LULC changes, the Land Change Modeler (LCM) in TerrSet (formerly known as IDRISI) software was developed [54,55]. LCM is an ArcGIS-integrated suite of tools for the assessment of future LULC changes, detecting gains and losses, net change, persistence, and identification of transitions between LULC classes [56]. To map future LULC scenarios, LCM utilizes historical LULC maps and a series of driving forces (Table 3). The Markov chain projection is performed by creating matrixes to estimate the transition probability and the area of each LULC class for future dates [57,58].

Table 3. Driving variables that were considered in the LCM simulations.

Driving Force	Type
Distance from disturbance	Dynamic
Distance from stream	Dynamic
Distance from urban	Dynamic
Distance from road	Dynamic
Evidence likelihood	Dynamic
Elevation	Static
Slope	Static

In this study, LCM was applied to forecast the future LULC in three scenarios (2030, 2040, 2050), via a few main steps: (i) analysis of historical LULC maps (1989, 2004, and 2019) and associated changes, (ii) creation of transition probability matrixes, (iii) model validation, iv) prediction of future LULC maps, accounting for possible driving forces. In this work, we define the probability transitional matrix as a matrix showing the transfer direction of LULC types from one category to other categories in a given year [10].

In LCM, there are two options for modeling algorithms that are used to model the transition variables: logistic regression and Multi-Layer Perceptron (MLP) neural network [59,60]. MLP uses minimal parameters, is more easily approachable, and has been extensively enhanced to offer an automatic mode that requires no user intervention. Therefore, in the present study, the MLP neural network has been employed.

To evaluate the capability of LCM in predicting future LULC, a predicted map of 2019 was created based on 1989 and 2004 LULC, and then compared with the actual 2019 map. To evaluate the quality of the 2019 predicted map against the 2019 reference map, the TerrSet validation module was used [61], mimicking the approach proposed in similar studies [62]. In TerrSet, two tools are available to assess the fit of the model to the sample data. First, the cross-validation tool iteratively removes a sample data point and interpolates a new value for the location. A table is produced to show the difference between the predicted attributes and the known attributes at those locations. Second, a variance image is produced that shows the spatial variation of uncertainty as a result of the fitted model. The variance image provides information to assist in identifying the problem areas where the relationship between the fitted model and the sample data points is poor [61].

Kappa indices, such as kappa for no information (*Kno*), kappa for location (*Klocation*), and kappa standards (*Kstandards*)l are used to identify potential errors [2,63,64]. Kappa values vary between 0 and 1, with values >0.8 meaning an almost perfect agreement. In detail, *Kstandards* is an index of agreement that attempts to account for the expected

agreement due to random spatial reallocation of the categories in the comparison map; *Kno* is identical to *Kstandards* if both the quantity and allocation of categories in the comparison map are selected randomly; *Klocation* represents the extent to which the maps agree in terms of location of each LULC category.

To corroborate the study outcomes, a series of statistics were considered [65]: agreement due to chance (agreement chance), agreement due to quantity (agreement quantity), agreement due to the location at the grid cell level (agreement grid cell), disagreement due to the location at the grid cell level (disagree grid cell), and disagreement due to quantity (disagree quantity) were calculated to indicate how well the comparison map agrees with the reference map [40].

Driving forces are the factors that affect LULC changes at the local scale, and therefore they should be locally investigated and addressed [8,66–68]. The driving variables (Table 3) were selected based on the actual literature and past studies, selecting the most important. In fact, there are still some other factors that are difficult to quantify, such as the population in the area. In simulating future LULC, LCM differentiates between static and dynamic variables, where the first are stable in time while the latter change temporally, and are therefore recalculated at each time step.

The type of land cover is strongly correlated with anthropogenic disturbance, for example, the local population can access resources more conveniently while changing the land use because of the distance from the stream. The ease with which land can transition to urban usage depends on the distance from urban centers, which can be a highly powerful force for change. One of the key factors in drawing more urban uses and expansion is the distance from roads, which determines accessibility. The primary topographic component known to affect LULC change is elevation. In addition, it seems reasonable to use the evidence likelihood, a quantitative variable that reflects the likelihood of discovering change between agricultural land and all other land classes at the relevant pixel, given that the annual pace of agricultural expansion was considerable. The watershed slope influences the spatial trends of land cover change, leading one to assume that changes in land use are highly influenced by the terrain slope: gains in urban land are primarily concentrated on relatively flat slopes and deforestation declines as the slope's gradient increases.

It is worth remembering that the selection of variables and indicators, to a certain extent, may cause some differences in the simulation results or model parameters, which will have effects on the prediction of LULC change. For example, for distance from the road, if the forest is very close to the road, the rate of forest clearance (deforestation) is very high, and vice versa, i.e., if there is road availability, the people living nearby can clear the forest for agriculture or other purposes. This is also applicable to other driving factors.

The Cramer's *V* Coefficient (*CVC*), sometimes called Cramer's *V* strategy [66], was used to assess the correlations between the various driving variables. In statistics, *CVC* is a measure of association between two categorical variables, giving a value between 0 and +1, and it is based on Pearson's chi-squared test [67]. According to Eastman [68], variables that have a Cramer's $V > 0.40$ are good and these drivers will have the greatest impact on the modification process and its spatial distribution [69–71]. One has to remember that *CVC* does not recognize interaction effects between the explanatory variables and land cover categories, while it only helps to determine whether to include a specific variable as a driving factor of LULC changes.

2.5. LULC Detection

LULC changes were detected via a few parameters: magnitude of change *C*, rate of change *R*, and change percentage *P*, using the following equations [2,72,73]:

$$C_i = L_i - B_i \tag{3}$$

$$R_i = \frac{L_i - B_i}{T} \tag{4}$$

$$P_i = \frac{L_i - B_i}{B_i} * 100 \quad (5)$$

where i represents the LULC class, B_i and L_i are the areas [ha] with the earliest and latter LULC, respectively. The period between B_i and L_i is T [year] and determines the rate of change R_i. Positive values of P_i mean an increase in a specific LULC in the study period T ($L_i > B_i$, $R_i > 0$), while negative values mean a decrease ($L_i < B_i$, $R_i < 0$).

3. Results

3.1. Historical LULC Maps

Three reference years (1989, 2004, and 2019) were considered to evaluate historical LULC via a maximum likelihood supervised classification (Figure 2). As reported in Table 4, in 1989 most of the study area was covered by agriculture (32%), grass/swamps (24%), and shrub (22%), with only a very minor part occupied by settlements (0.4%). Similar LULC was observed in 2004, with agriculture (34%), grass/swamp (24%), and shrub (18%) being the most dominant LULC classes and just a small increase in the area covered by built-up (1%). In 2019, the class distribution remained similar, with an increase in the built-up area (1.7%). In summary, in the past, agriculture was always the most dominant LULC class in the Fincha watershed, followed by grass/swamp and shrub.

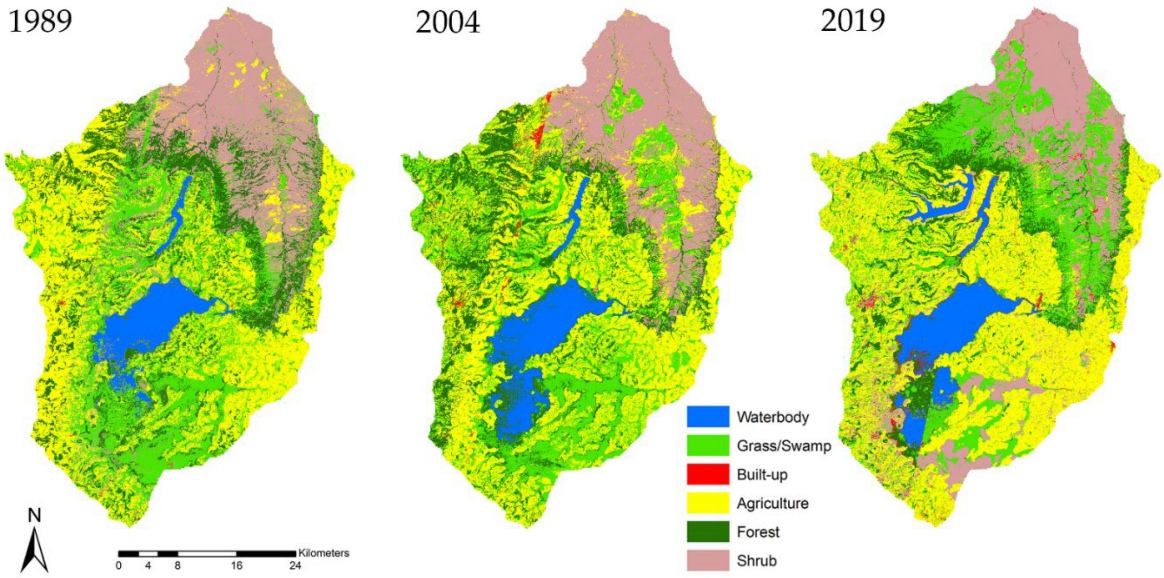

Figure 2. LULC maps of the Fincha watershed in the three reference years.

Table 4. Details of LULC area of the Fincha watershed in the three reference years.

LULC Type	1989		2004		2019	
	[ha]	[%]	[ha]	[%]	[ha]	[%]
Waterbody	15,744.08	5.24	19,928.15	6.63	20,860.55	6.94
Grass/Swamp	73,371.25	24.42	73,423.56	24.43	73,570.49	24.48
Built-up	1252.00	0.42	2945.40	0.98	5007.75	1.67
Agriculture	96,966.71	32.27	103,033.14	34.29	115,446.96	38.42
Forest	48,373.16	16.10	46,569.29	15.50	29,213.93	9.72
Shrub	64,790.11	21.56	54,597.77	18.17	56,397.63	18.77
Total	30,0497.31	100.00	30,0497.31	100.00	300,497.31	100.00

The results reported in Figure 2 are in agreement with Dibaba et al. [39], who pointed out that the Fincha watershed is characterized by an expansion of agriculture and built-up LULC, resulting in a decline of natural vegetation.

3.2. Accuracy Assessment for Historical LULC

The overall accuracies *OA* and kappa values *K* were 82.80%, 85.57%, and 89.82% and 80.51%, 82.54%, and 87.84%, respectively, for the three reference years (Tables 5 and A1, Tables A2 and A3). These results indicate that the accuracy of the classifications improved from 1989 to 2019, also thanks to the higher quality of the satellite data used.

Table 5. LULC classification accuracy for 1989, 2004, and 2019.

Year	LULC Class	Producer Accuracy	User Accuracy	OA [%]	K [%]
1989	Waterbody	92.86	89.66	82.80	80.51
	Grass/Swamp	76.78	86.00		
	Built-up	84.61	84.62		
	Agriculture	82.69	74.14		
	Forest	85.71	87.80		
	Shrub	80.43	80.43		
2004	Waterbody	97.06	91.67	85.57	82.54
	Grass/Swamp	75.14	84.13		
	Built-up	83.87	86.67		
	Agriculture	88.41	81.33		
	Forest	89.80	93.62		
	Shrub	84.62	81.48		
2019	Waterbody	94.44	85.00	89.82	87.84
	Grass/Swamp	86.30	87.50		
	Built-up	97.14	91.89		
	Agriculture	90.45	95.00		
	Forest	89.29	92.59		
	Shrub	86.67	85.25		

The accuracy of a map could be different for users and map developers. The user's accuracy indicates how often a specified class on the map is present on the ground, while the producer's (mapmaker) accuracy shows the probability that a certain land cover is classified according to field evidence.

Hailu et al. [40] defined the kappa statistics <40%, 40–75%, and >75% as poor, good, and excellent, respectively. Using this approach, from Table 5 one can notice that the statistics of the Fincha watershed were excellent, meaning a very good agreement between the classification maps and the reference information.

3.3. Historical LULC Changes and Transition Probability Matrix

Comparing the three reference years, it is possible to observe a considerable reduction in the area covered by forest and shrubs during the observation period (Table 6). In detail, yearly, around 639 ha of forest and 280 ha of shrubs were cleared in favor of other LULC classes. As anticipated, human pressure contributed to changing the environment, as recognizable by the increase in areas covered by agricultural fields, built-up, grass/swamp, and waterbodies, which yearly gained around 616 ha, 125 ha, 7 ha, and 171 ha, respectively. Waterbodies increased significantly during the last 30 years, mainly because of human intervention. In fact, in 1989, the Amerti reservoir, one of the reservoirs located in the Fincha watershed, was not filled, while it was filled in 2004. In 2019, another dam was constructed over the Nashe River [2]. The study pointed out small changes in terms of grass/swamps, at least in terms of net variation. In fact, as is visible from Figure 3 and Table 6, the majority of the Fincha watershed was affected by variations in LULC that include this class.

The results presented here are in line with the existing literature on LULC in the Fincha watershed [17,39]. All the authors agreed that the shift from natural LULC towards more anthropized environments could threaten biodiversity and decrease the total values of ecosystem services [74].

Table 6. Historical LULC changes in the Fincha watershed.

LULC Class	1989–2004			2004–2019			1989–2019		
	Area [ha]	Area [%]	Change [ha/Year]	Area [ha]	Area [%]	Change [ha/Year]	Area [ha]	Area [%]	Change [ha/Year]
Agriculture	6067.5	6.3	404.5	12,412.7	12.1	827.5	18,480.3	19.06	616.0
Built-up	1693.4	135.3	112.9	2062.3	70.0	137.5	3755.8	300.0	125.2
Forest	−1803.9	−3.7	−120.3	−17,355.4	−37.3	−1157.0	−19,159.2	−39.6	−638.6
Grass/Swamps	52.3	0.1	3.5	146.9	0.2	9.8	199.2	0.3	6.6
Shrub	−10,192.3	−15.7	−679.5	1799.9	3.3	120.0	−8392.5	−13.0	−279.8
Waterbody	4183.0	26.6	278.9	933.4	4.7	62.2	5116.3	32.5	170.5

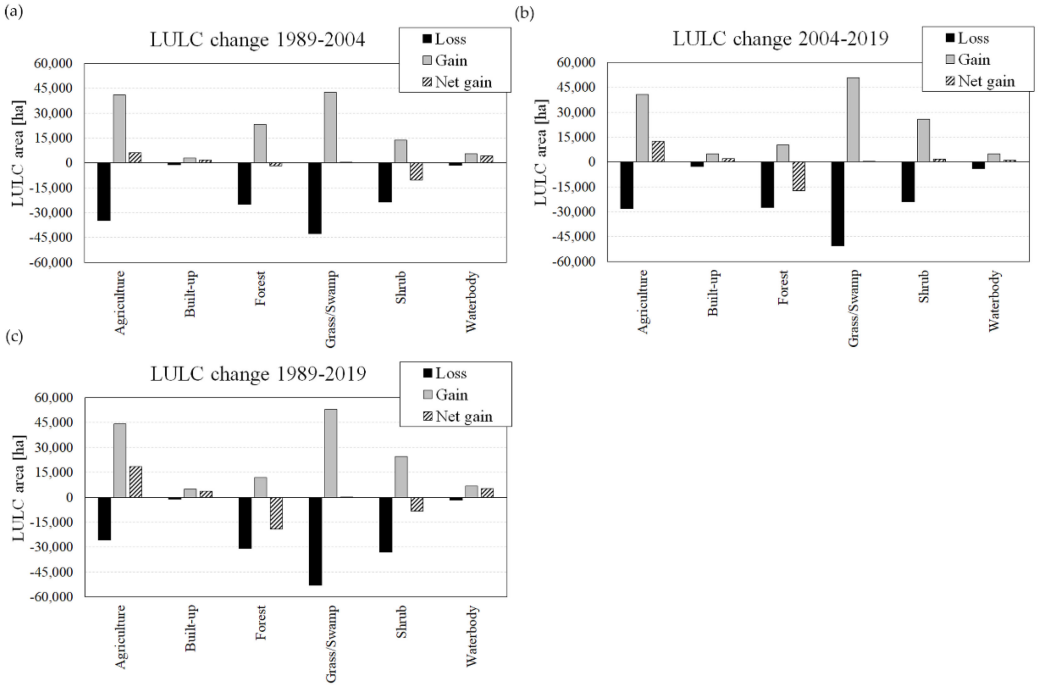

Figure 3. LULC changes during the observed period: (**a**) from 1989 to 2004, (**b**) from 2004 to 2019, (**c**) from 1989 to 2019.

It is worth recalling that the probability transitional matrix is the transfer direction of LULC types from one category to other categories in the given year [10]. The nature change can be distinguished from the Markov transitional matrices for historical LULC over the period (1989–2004 and 2004–2019). The nature of change can be distinguished from the trend as depicted in the Markov transition matrices over the period between 1989 and 2019. The diagonal values represent the probability that each land cover class remains persistent (constant) from earlier to later years. The other values represent a given land cover land class undertaking transition to another land cover land class.

Between 1989 and 2004, the highest and the lowest persistent LULC classes were waterbody and grass/swamps, characterized by a percentage of stability of 91% and 42%, respectively. During the period 2004–2019, the most and the least stable LULC class categories were waterbody and grass/swamp, which accounted for around 80% and 31%, respectively. Over the entire temporal horizon observed (1989 to 2019), a large part of the forest was converted to agriculture and grass/swamps (see Tables A4–A6 for the detailed LULC transition matrixes).

According to information obtained during field investigations (KII and field evidence), waterbodies increased after the construction of the Nashe Dam. During the construction of the reservoir, many farmers along and downstream of the Nashe stream were displaced to other agricultural places or towns. The abandonment of fields and the need for resettling

in other areas caused a decrease in forests and an increase in built-up areas. In addition, poorly planned and long-term urban development and agricultural management strategies contribute to negatively affecting natural resources, causing a significant decline in the last decades (Figure 3).

3.4. Model Validation

The LULC map of 2019, predicted from the 1989 and 2004 data, has been validated with the classified LULC map of the very same year (Table 7), showing that the LCM model can effectively forecast LULC changes.

Table 7. LULC classes in 2019: projected vs classified values.

	LCM Projected LULC		Classified LULC	
LULC Class	**Area [ha]**	**Percentage [%]**	**Area [ha]**	**Percentage [%]**
Waterbody	19,942.55	6.64	20,861.54	6.94
Grass/swamp	76,883.19	25.58	73,570.84	24.48
Built-up	3007.232	1.00	5007.76	1.67
Agriculture	108,578.3	36.13	115,449.74	38.42
Forest	48,717.03	16.21	29,214.18	9.72
Shrub	43,377.06	14.43	56,401.33	18.77
Total	300,505.4	100.00	300,505.40	100.00

The capability of LCM in predicting the 2019 LULC was assessed via *K*-indexes and other statistics in TerrSet (Table 8). All the values of the computed *K*-indexes (>80%) indicate good agreement between the projected and the actual LULC map [2]. The Disagree Quantity (0.0742) is greater than the Disagree Gridcell (0.0268), indicating that the model has a higher ability to predict the LULC in location (spatial) than in quantity for the Fincha watershed.

Table 8. Results of using the Multi-Layer Perceptron Markov Chain (MLP_MC) model for predicting LULC in 2019.

Statistics	**Value**
Kno	0.8743
Klocation	0.8864
Kstandards	0.8285
Agreement Chance	0.1667
Agreement Quantity	0.3252
Agreement Gridcell	0.4071
Disagreement Gridcell	0.0268
Disagreement Quantity	0.0742

3.5. Future LULC

To forecast future LULC changes, it is necessary to account for the most important driving variables (Table 9). As shown, all variables but the slope should be included in LCM, as the Cramer's *V* value of the slope is very low.

Table 9. Cramer's *V* values of driving forces.

Driving Force	**Cramer's V Value**
Distance from disturbance	0.2782
Distance from stream	0.3240
Distance from urban	0.1548
Distance from road	0.2736
Evidence likelihood	0.4212
Elevation	0.2949
Slope	0.0101

The LULC maps for 2030, 2040, and 2050 were created via LCM, using the historical maps as a basis (Figure 4). As observed in the past, an increase in areas covered by agriculture, built-up, grass/swamp, and waterbody is forecast, while a drastic decrease in forest and shrub should be expected, with a slower rate of deforestation in the decade 2040–2050 (Figure 5 and Table 10). The decrease in natural forests, in combination with climate change, is likely to negatively affect the hydrological cycle of the whole Fincha sub-basin, as already shown by preliminary studies [7]. Moreover, the lower availability of wood (mostly timber) for construction will also impact the local economy.

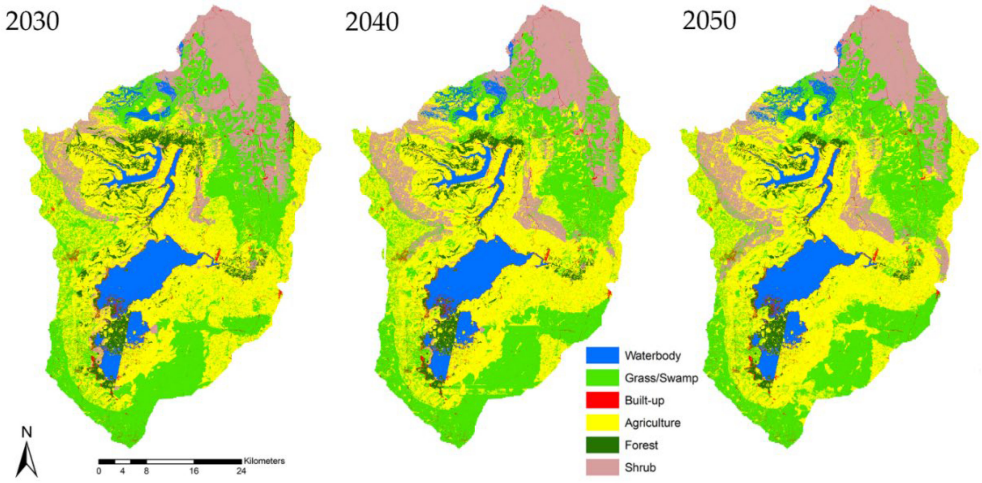

Figure 4. Predicted LULC of the Fincha watershed for the next three decades.

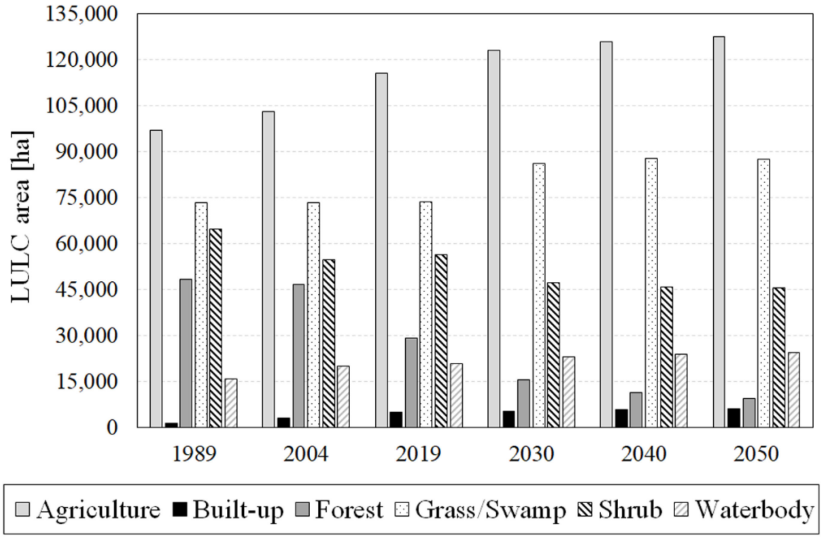

Figure 5. Observed (1989, 2004, 2019) and simulated (2030, 2040, 2050) LULC in the Fincha watershed.

Table 10. Future LULC changes in the Fincha watershed.

	2019–2030		2030–2040		2040–2050		2019–2050	
LULCC Class	**[ha]**	**[%]**	**[ha]**	**[%]**	**[ha]**	**[%]**	**[ha]**	**[%]**
Agriculture	7722.2	6.7	2795.1	2.3	1619	1.3	12,136.3	10.5
Built-up	358.8	7.2	420.7	7.8	204.5	3.5	984	19.6
Forest	−13,585.1	−46.5	−4374.9	−28.0	−1808.4	−16.1	−19,768.4	−67.7
Grass/swamp	12,589	17.1	1672.5	1.9	−235.5	−0.3	14,026	19.1
Shrub	−9287.6	−16.5	−1309.8	−2.8	−392.8	−0.9	−10,990.2	−19.5
Waterbody	2204.5	10.6	796.3	3.5	613.1	2.6	3613.9	17.3

In terms of transition probability (Tables A7–A9), areas covered by forest and shrubs are more prone to be converted into agricultural land, while built-up areas should be expected on the grass/swamp zones. This indicates that, in the future, agriculture and built-up zones will expand at a high rate since the other LULC classes will be converted to them. Conversely, forests and shrubs will decline at a significant rate.

4. Discussion and Policy Implications

As suggested in the review carried out by Regasa et al. [3], most of the studies of LULC in Ethiopia are on a local scale, analyzing how past variations affected water resources and socio-economic conditions in the region. This was mostly connected with the difficulty in obtaining proper field evidence (e.g., photos, description of LULC changes observed by local inhabitants). Therefore, very few works tried to forecast future LULC changes at the watershed scale, eventually providing new insights that can be useful for developing future basin-wide management strategies [74]. The present study was developed to fill this gap, estimating the Fincha sub-basin LULC for the next three decades (2030, 2040, and 2050) based on past information (LULC in 1989, 2004, and 2019), to infer trends to be used in multiple ways. The LCM results point out that, in the coming decades, significant changes in LULC should be expected, mostly because of the ever-increasing pressure of humans in need of more land for settlements and cropland. Indeed, the local population is growing, and more natural resources are needed to satisfy their needs for food, energy, and construction materials [2,7,75–77]. Apart from the direct consequences on the environment, the ongoing deforestation in the Fincha sub-basin is also causing an intensification of soil erosion, triggering sediment siltation in the various reservoirs located in the region, eventually leading to a decrease in reservoir efficiency in terms of water availability and hydropower production. Therefore, future studies should integrate the analysis of LULC changes with the simulation of soil erosion and sediment transport, to help local authorities better plan adequate management strategies to reduce siltation and guarantee the sustainability of local water resources, biodiversity, and socio-economy.

The reduction in forest cover pointed out in the present study compares well with similar research performed at the Ethiopian level [2,7,17,28,39,74,78–80]. This trend was historically caused by the political situation, as, during the 1970s, the military regime proclaimed the nationalization of all rural land, abolishing private property [28,75,81,82]. However, the state was unable to adequately manage the land, and the majority of the forest was converted to settlements, agricultural land, and highly degraded areas because of the low level of land management practices. A similar approach has been taken since, but nowadays the land is property of the nations, nationalities, and people of Ethiopia according to Article 40(3) of the constitution endorsed in 1994 [83]. Because of the present policies, an increasing number of farmers are pushing for the expansion of their fields at the expense of the natural environment, in search of better socio-economic conditions driven by market-oriented choices [84–86].

As pointed out by Tolessa et al. [86], the reduction in land coverage and ecosystem services connected to natural resources such as forests are strictly connected with the present policy. As also shown in past investigation [87] and in the present work, the trend of decreasing forests to provide room for agriculture is very likely to continue in the future, also following the Ethiopian legislation. In fact, in Ethiopia, farmers have more legal rights over their land if they convert forest land into farmland, as the law stipulates natural forests as the property of the government. This forces farmers (legally or illegally) to convert forests into agricultural areas, as this guarantees them the use of the land for an indefinite period. As in other Ethiopian watersheds, the Fincha sub-basin was also affected by the 1975 land reform as, after it, grazing lands and forests were freely accessed for various uses. Tefera and Sterk [88] showed that, of the land potentially available for community use, cropland covered 77% of the whole region in 2001, indicating that further expansion cannot accommodate new farm families. This corroborates the hypotheses made in the present work, where future LULC was simulated assuming a trend similar to recent decades.

As with other Ethiopian basins [89], in the Fincha sub-basin, population pressure is a top driver of LULC change. To address this, in addition to policy changes, the local community should also start reforestation of the degraded forest area to assure the sustainability of the environment in the future, as also stressed by Senbeta [90].

To provide both decision-makers and local stakeholders such as farmers with more evidence on the importance of safeguarding water resources and ecosystem services at the basin scale, additional studies are needed, also taking advantage of information remotely acquired, such as satellite imagery, or considering different simulation algorithms and expanding the dataset of field evidence. Indeed, acquiring ground truth data and information from the local population, paramount for assuring a proper calibration/validation of the model, in locations that are hardly reachable or with unstable political situations such as the Fincha sub-basin, could be very difficult and expensive.

5. Conclusions

The present study investigated the historical LULC (years 1989, 2004, and 2019) in the Ethiopian Fincha watershed via a combination of satellite imagery and field support data. Based on such analysis, the Land Change Modeller was applied to forecast LULC over the next three decades (years 2030, 2040, and 2050). The 2019 LULC map was used for validating the LCM approach, comparing the forecast situation with the actual one derived from satellite images, indicating that the used Multi-Layer Perceptron (MLP) neural network of Markov chain (MC) has enough capability to predict future LULC.

The study results have shown that, over the last thirty years, the forest covering the Fincha watershed was mostly converted to agricultural and grass/swamp areas. An increase in zones covered by waterbody and built-up was also observable, mainly connected to the increasing human pressure and the construction of new hydropower reservoirs. This trend is recognizable not only in the study sub-basin but also in many Ethiopian basins [3], showing that LULC changes represent a major problem in the country.

As pointed out by the modeling results, in the future, a similar trend is more than probable. Indeed, if management strategies are not changed towards a more sustainable approach, also via proper reforms at the national level, an even more significant decrease in forest coverage should be expected in favor of new settlement areas and cropland. This change could help locals in sustaining their livelihood in the short term, but, in the medium/long term, the reduction in areas covered by forest will contribute to decreasing biodiversity and ecosystem services, as well as fostering soil erosion, with detrimental consequences such as reservoir siltation.

It is worth remembering that, to corroborate the results presented here and to reduce the uncertainties, additional data should be included in the study, mostly deriving from laborious and expensive field investigations. However, due to the current conditions of the study area, obtaining such information in the coming months could be very challenging. On the other hand, the increasing availability of commercial high-resolution satellite images could partially help in enlarging the dataset of field evidence, pointing out LULC changes happening at a more detailed scale. Therefore, in the future, a deeper analysis of satellite information is planned.

Author Contributions: Conceptualization, M.S.R. and M.N.; writing-original draft preparation, M.S.R. and M.N.; writing-review, M.S.R. and M.N.; literature review, M.S.R. and M.N.; supervision, M.N.; project administration, M.N.; funding acquisition, M.N. All authors have read and agreed to the published version of the manuscript.

Funding: This research was funded by NCN National Science Centre Poland–call PRELUDIUM BIS-1, Grant Number 2019/35/O/ST10/00167. Project website: https://sites.google.com/view/lulc-fincha/home (accessed on 1 June 2022).

Institutional Review Board Statement: Not applicable.

Informed Consent Statement: Not applicable.

Data Availability Statement: Additional data are available from the corresponding author, and partially available at https://dataportal.igf.edu.pl/dataset/land-use-land-cover-changes-percentage-in-ethiopia (accessed on 1 June 2022).

Acknowledgments: A great thank you goes to all the authorities and stakeholders involved in the field survey, which was paramount for validating our results. Moreover, we would like to thank the three anonymous reviewers for their useful comments, which helped us to better detail our research. We also thank the editors for their work in handling our manuscript and the revision process.

Conflicts of Interest: The authors declare no conflict of interest.

Appendix A. Accuracy Assessment of Historical LULC

The accuracy of the historical maps of LULC was assessed separately, showing the following results:

Table A1. Overall accuracy and kappa statistics for 1989.

LULC Class	Waterbody	Grass/Swamp	Built-Up	Agriculture	Forest	Shrub	Total	Users Accuracy [%]
Waterbody	26	3	0	0	0	0	29	89.66
Grass/swamp	1	43	1	3		2	50	86.00
Built-up	0	1	22	2	1	0	26	84.62
Agriculture	0	7	3	43	2	3	58	74.14
Forest	0	0	0	1	36	4	41	87.80
Shrub	1	2	0	3	3	37	46	80.43
Total	28	56	26	52	42	46	250	
Producer's accuracy	92.86	76.78	84.61	82.69	85.71	80.43		82.80

Table A2. Overall accuracy and kappa statistics for 2004.

LULC Class	Waterbody	Grass/Swamp	Built-Up	Agriculture	Forest	Shrub	Total	Users Accuracy [%]
Waterbody	33	3	0	0	0	0	36	91.67
Grass/swamp	0	53	1	6	0	3	63	84.13
Built-up	0	2	26	1	1	0	30	86.67
Agriculture	0	7	3	61	1	3	75	81.33
Forest	0	1	0	0	44	2	47	93.62
Shrub	1	4	1	1	3	44	54	81.48
Total	34	70	31	69	49	52	305	
Producer's accuracy	97.06	75.14	83.87	88.41	89.80	84.62		85.57

Table A3. Overall accuracy and kappa statistics for 2019.

LULC Class	Waterbody	Grass/Swamp	Built-Up	Agriculture	Forest	Shrub	Total	Users Accuracy [%]
Waterbody	34	3	0	0	3	0	40	85
Grass/swamp	2	63	0	4	0	3	72	87.5
Built-up	0	0	34	1	1	1	37	91.89
Agriculture	0	2	1	76	0	1	80	95
Forest	0	1	0	0	50	3	54	92.59
Shrub	0	4	0	3	2	52	61	85.25
Total	36	73	35	84	56	60	344	
Producer's accuracy	94.44	86.30	97.14	90.45	89.29	86.67		89.82

Appendix B. Transition Matrixes Historical LULC

Tables A4–A6 summarize the transition matrix between the three reference years. Detailed analysis and a discussion of these results are reported in Section 3.3.

Table A4. Transition area matrix [ha] from 1989 to 2004.

Land Class		2004						Total	Percentage of Stability (%)
		Agriculture	Built-Up	Forest	Grass/Swamp	Shrub	Waterbody		
1989	Agriculture	62,112.6	607.9	9025.1	21,434.4	3434.4	352.4	96,966.7	64.5
	Built-up	514.5	704.0	184.2	258.0	220.0	5.0	1252.0	56.0
	Forest	6325.0	875.4	23,355.9	11,338.0	4857.3	1621.6	48,373.2	48.3
	Grass/Swamp	24,120.9	412.2	10,034.8	30,765.4	5016.3	3021.9	73,371.3	41.9
	Shrub	9956.4	972.9	2872.0	9370.6	41,011.7	606.6	64,790.1	63.3
	Waterbody	3.8	6.7	1097.3	257.3	58.2	14,320.8	15,744.1	91.0
	Total	103,033.1	2945.4	46,569.3	73,423.6	54,597.8	19,928.2	300,497.3	

Table A5. Transition area matrix [ha] from 2004 to 2019.

Land Class		2019						Total	Percentage of Stability (%)
		Agriculture	Built-Up	Forest	Grass/Swamp	Shrub	Waterbody		
2004	Agriculture	74,841.6	1627.9	1405.5	14511.7	10,274.4	373.1	103,034.3	72.6
	Built-up	350.0	1024.0	720.3	1208.1	554.4	10.2	2945.4	34.8
	Forest	7476.7	1034.5	19,066.9	14,450.5	2202.5	2338.2	46,569.2	40.9
	Grass/Swamp	30,227.2	979.7	4619.3	22,820.6	12,648.9	2128.0	73,423.5	31.1
	Shrub	2540.9	645.2	1776.3	19,004.0	30,591.5	39.82	54,597.7	56.0
	Waterbody	10.6	618.0	1625.6	1575.7	126.0	15,972.2	19,928.2	80.1
	Total	115,447.0	5007.8	29,213.9	73,570.5	56,397.6	20,861.5	300,498.3	

Table A6. Transition area matrix [ha] from 1989 to 2019.

Land Class		2019						Total	Percentage of Stability (%)
		Agriculture	Built-Up	Forest	Grass/Swamp	Shrub	Waterbody		
1989	Agriculture	71,320.09	1517.76	1965.61	13,597.53	8041.16	528.00		78.2
	Built-up	422.17	77.11	108.22	314.58	322.98	6.92	1251.98	95.7
	Forest	7954.91	801.46	17,400.68	16,309.28	4393.61	1513.61	48,373.55	52.6
	Grass/Swamp	30,733.54	1185.15	5318.34	20,417.33	11,716.12	4002.57	73,373.05	57.9
	Shrub	4998.46	954.23	3678.88	22,463.67	31,882.18	816.55	64,793.97	65.8
	Waterbody	21.35	472.00	742.95	470.60	43.29	13993.88	15744.07	100.0
	Total	115,450.52	5007.71	29,214.66	73,572.99	56,399.35	20,861.54	300,506.76	

Appendix C. Transition Matrices for Future LULC

Tables A7–A9 summarize the transition matrix of the forecasted LULC (see Section 3.5).

Table A7. Transition area matrix [ha] of LULC from 2019 to 2030.

Land Class		2030						Total	Percentage of Stability (%)
		Agriculture	Built-Up	Forest	Grass/Swamp	Shrub	Waterbody		
2019	Agriculture	90,279.1	52.3	35.3	15,280.6	9798.9	0.0	115,446.2	78.2
	Built-up	95.3	4789.8	0.00	120.9	1.7	0.0	5007.8	95.7
	Forest	3154.1	3.26	15,357.8	9425.6	44.7	1228.6	29,214.1	52.6
	Grass/Swamp	29,051.8	508.2	233.7	42,631.3	171.8	972.6	73,569.3	57.9
	Shrub	588.9	13.1	2.0	18,701.0	37,093.0	3.3	56,401.1	65.8
	Waterbody	0.00	0.00	0.00	0.00	0.00	20,861.5	20,861.5	100.0
	Total	123,169.2	5366.6	15,628.8	86,159.5	47,110.0	23,066.0	300,499.9	

Table A8. Transition area matrix [ha] of LULC from 2030 to 2040.

Land Class		2040						Total	Percentage of Stability (%)
		Agriculture	Built-Up	Forest	Grass/Swamp	Shrub	Waterbody		
2030	Agriculture	110,334.9	22.5	19.2	6339.8	6268.9	183.9	123,169.2	89.6
	Built-up	47.8	5268.5	0.0	39.6	10.6	0.2	5366.6	98.2
	Forest	830.1	0.6	11,219.3	3565.6	8.6	4.6	15,628.8	71.8
	Grass/Swamp	10986.0	467.1	3.6	73,678.3	186.5	838.0	86,159.5	85.5
	Shrub	3530.6	28.5	11.8	4195.6	39,320.3	23.2	47,110.0	83.5
	Waterbody	234.9	0.0	0.0	13.1	5.5	22,812.5	23,066.0	98.9
	Total	125,964.28	5787.3	11,253.9	87,832.0	45,800.2	23,862.3	300,499.9	

Table A9. Transition area matrix [ha] of LULC from 2040 to 2050.

Land Class		2050						Total	Percentage of Stability (%)
		Agriculture	Built-Up	Forest	Grass/Swamp	Shrub	Waterbody		
2040	Agriculture	118,408.7	17.5	10.8	3481.5	3838.9	207.0	125,964.3	94.0
	Built-up	28.2	5722.2	0.0	33.8	2.8	0.3	5787.3	98.9
	Forest	42.8	0.2	9430.3	1780.3	0.4	0.0	11,253.9	83.8
	Grass/Swamp	8347.1	242.7	2.4	78,766.4	53.6	419.7	87,832.0	89.7
	Shrub	746.2	9.2	2.1	3521.6	41,509.3	11.9	45,800.2	90.6
	Waterbody	10.3	0.0	0.0	12.9	2.4	23,836.6	23,862.3	99.9
	Total	127,583.3	5991.8	9445.5	87,596.5	45,407.4	24,475.4	300,499.9	

References

1. Alam, A.; Bhat, M.S.; Maheen, M. Using Landsat satellite data for assessing the land use and land cover change in Kashmir valley. *GeoJournal* **2020**, *85*, 1529–1543. [CrossRef]
2. Leta, M.K.; Demissie, T.A.; Tränckner, J. Hydrological Responses of Watershed to Historical and Future Land Use Land Cover Change Dynamics of Nashe Watershed, Ethiopia. *Water* **2021**, *13*, 2372. [CrossRef]
3. Regasa, M.S.; Nones, M.; Adeba, D. A Review on Land Use and Land Cover Change in Ethiopian Basins. *Land* **2021**, *10*, 585. [CrossRef]
4. Tadese, S.; Soromessa, T.; Bekele, T. Analysis of the current and future prediction of land use/land cover Change using remote sensing and the CA-markov model in majang forest biosphere reserves of Gambella, southwestern Ethiopia. *Sci. World J.* **2021**, *2021*, 6685045. [CrossRef]
5. Dwivedi, R.S.; Sreenivas, K.; Ramana, K.V. Cover: Land-use/land-cover change analysis in part of Ethiopia using Landsat Thematic Mapper data. *Int. J. Remote Sens.* **2005**, *26*, 1285–1287. [CrossRef]
6. Demissie, T.A. Land use and land cover change dynamics and its impact on watershed hydrological parameters: The case of Awetu watershed, Ethiopia. *J. Sediment. Environ.* **2022**, *7*, 79–94. [CrossRef]
7. Kenea, U.; Adeba, D.; Regasa, M.S.; Nones, M. Hydrological Responses to Land Use Land Cover Changes in the Fincha'a Watershed, Ethiopia. *Land* **2021**, *10*, 916. [CrossRef]
8. Khan, T.U.; Mannan, A.; Hacker, C.E.; Ahmad, S.; Amir Siddique, M.; Khan, B.U.; Luan, X. Use of GIS and Remote Sensing Data to Understand the Impacts of Land Use/Land Cover Changes (LULCC) on Snow Leopard (*Panthera uncia*) Habitat in Pakistan. *Sustainability* **2021**, *13*, 3590. [CrossRef]
9. Lambin, E.F.; Rounsevell, M.D.; Geist, H.J. Are agricultural land-use models able to predict changes in land-use intensity? *Agric. Ecosyst. Environ.* **2000**, *82*, 321–331. [CrossRef]
10. Han, H.; Yang, C.; Song, J. Scenario simulation and the prediction of land use and land cover change in Beijing, China. *Sustainability* **2015**, *7*, 4260–4279. [CrossRef]
11. Rahman, M.T.U.; Tabassum, F.; Rasheduzzaman, M.; Saba, H.; Sarkar, L.; Ferdous, J.; Islam, A.Z. Temporal dynamics of land use/land cover change and its prediction using CA-ANN model for southwestern coastal Bangladesh. *Environ. Monit. Assess.* **2017**, *189*, 565. [CrossRef]
12. Fan, F.; Wang, Y.; Wang, Z. Temporal and spatial change detecting (1998–2003) and predicting of land use and land cover in Core corridor of Pearl River Delta (China) by using TM and ETM+ images. *Environ. Monit. Assess.* **2008**, *137*, 127–147. [CrossRef]
13. Girma, R.; Fürst, C.; Moges, A. Land use land cover change modeling by integrating artificial neural network with cellular Automata-Markov chain model in Gidabo river basin, main Ethiopian rift. *Environ. Chall.* **2022**, *6*, 100419. [CrossRef]
14. Gupta, R.; Sharma, L.K. Efficacy of Spatial Land Change Modeler as a forecasting indicator for anthropogenic change dynamics over five decades: A case study of Shoolpaneshwar Wildlife Sanctuary, Gujarat, India. *Ecol. Indic.* **2020**, *112*, 106171. [CrossRef]

15. Getachew, D.; Kaur, R. Modeling Land-Use/Land-Cover Change, Using Multi-Layer Perceptron and Markov Chain Analysis: A Study on Bahir Dar City, Ethiopia. In *Re-Envisioning Remote Sensing Applications*; CRC Press: Boca Raton, FL, USA, 2021; pp. 241–260.
16. Etemadi, H.; Smoak, J.M.; Karami, J. Land use change assessment in coastal mangrove forests of Iran utilizing satellite imagery and CA–Markov algorithms to monitor and predict future change. *Environ. Earth Sci.* **2018**, *77*, 208. [CrossRef]
17. Leta, M.K.; Demissie, T.A.; Tränckner, J. Modeling and Prediction of Land Use Land Cover Change Dynamics Based on Land Change Modeler (LCM) in Nashe Watershed, Upper Blue Nile Basin, Ethiopia. *Sustainability* **2021**, *13*, 3740. [CrossRef]
18. Al-sharif, A.A.; Pradhan, B. Monitoring and predicting land use change in Tripoli Metropolitan City using an integrated Markov chain and cellular automata models in GIS. *Arab. J. Geosci.* **2014**, *7*, 4291–4301. [CrossRef]
19. Subedi, P.; Subedi, K.; Thapa, B. Application of a hybrid cellular automaton–Markov (CA-Markov) model in land-use change prediction: A case study of Saddle Creek Drainage Basin, Florida. *Appl. Ecol. Environ. Sci.* **2013**, *1*, 126–132. [CrossRef]
20. Mondal, M.S.; Sharma, N.; Garg, P.K.; Kappas, M. Statistical independence test and validation of CA Markov land use land cover (LULC) prediction results. *Egypt. J. Remote Sens. Space Sci.* **2016**, *19*, 259–272. [CrossRef]
21. Baig, M.F.; Mustafa, M.R.; Baig, I.; Takaijudin, H.B.; Zeshan, M.T. Assessment of land use land cover changes and future predictions using CA-ANN simulation for Selangor, Malaysia. *Water* **2022**, *14*, 402. [CrossRef]
22. Daba, M.H.; You, S. Quantitatively assessing the future land-use/land-cover changes and their driving factors in the upper stream of the Awash River based on the CA–Markov model and their implications for water resources management. *Sustainability* **2022**, *14*, 1538. [CrossRef]
23. Wu, F.; Mo, C.; Dai, X. Analysis of the Driving Force of Land Use Change Based on Geographic Detection and Simulation of Future Land Use Scenarios. *Sustainability* **2022**, *14*, 5254. [CrossRef]
24. Naikoo, M.W.; Rihan, M.; Peer, A.H.; Talukdar, S.; Mallick, J.; Ishtiaq, M.; Rahman, A. Analysis of peri-urban land use/land cover change and its drivers using geospatial techniques and geographically weighted regression. *Environ. Sci. Pollut. Res.* **2022**, 1–9. [CrossRef]
25. Kafy, A.A.; Naim, N.H.; Khan, M.H.H.; Islam, M.A.; Al Rakib, A.; Al-Faisal, A.; Sarker, M.H.S. Prediction of urban expansion and identifying its impacts on the degradation of agricultural land: A machine learning-based remote-sensing approach in Rajshahi, Bangladesh. In *Re-Envisioning Remote Sensing Applications*; CRC Press: Boca Raton, FL, USA, 2021; pp. 85–106. [CrossRef]
26. Hoque, M.Z.; Islam, I.; Ahmed, M.; Hasan, S.S.; Prodhan, F.A. Spatio-temporal changes of land use land cover and ecosystem service values in coastal Bangladesh. *Egypt. J. Remote Sens. Space Sci.* **2022**, *25*, 173–180.
27. Roy, A.; Inamdar, A.B. Multi-temporal Land Use Land Cover (LULC) change analysis of a dry semi-arid river basin in western India following a robust multi-sensor satellite image calibration strategy. *Heliyon* **2019**, *5*, e01478. [CrossRef]
28. Reid, R.S.; Kruska, R.L.; Muthui, N.; Taye, A.; Wotton, S.; Wilson, C.J.; Mulatu, W. Land-use and land-cover dynamics in response to changes in climatic, biological and socio-political forces: The case of southwestern Ethiopia. *Landsc. Ecol.* **2000**, *15*, 339–355. [CrossRef]
29. Govender, T.; Dube, T.; Shoko, C. Remote sensing of land use-land cover change and climate variability on hydrological processes in Sub-Saharan Africa: Key scientific strides and challenges. *Geocarto Int.* **2022**, 1–25. [CrossRef]
30. Mussa, M.; Teka, H.; Mesfin, Y. Land use/cover change analysis and local community perception towards land cover change in the lowland of Bale rangelands, Southeast Ethiopia. *Int. J. Biodivers. Conserv.* **2017**, *9*, 363–372.
31. Näschen, K.; Diekkrüger, B.; Evers, M.; Höllermann, B.; Steinbach, S.; Thonfeld, F. The impact of land use/land cover change (LULCC) on water resources in a tropical catchment in Tanzania under different climate change scenarios. *Sustainability* **2019**, *11*, 7083. [CrossRef]
32. Kuma, H.G.; Feyessa, F.F.; Demissie, T.A. Land-use/land-cover changes and implications in Southern Ethiopia: Evidence from remote sensing and informants. *Heliyon* **2022**, *8*, e09071. [CrossRef]
33. Tolessa, T.; Senbeta, F.; Kidane, M. The impact of land use/land cover change on ecosystem services in the central highlands of Ethiopia. *Ecosyst. Serv.* **2017**, *23*, 47–54. [CrossRef]
34. Shiferaw, H.; Bewket, W.; Alamirew, T.; Zeleke, G.; Teketay, D.; Bekele, K.; Eckert, S. Implications of land use/land cover dynamics and Prosopis invasion on ecosystem service values in Afar Region, Ethiopia. *Sci. Total Environ.* **2019**, *675*, 354–366. [CrossRef] [PubMed]
35. Biratu, A.A.; Bedadi, B.; Gebrehiwot, S.G.; Melesse, A.M.; Nebi, T.H.; Abera, W.; Egeru, A. Ecosystem Service Valuation along Landscape Transformation in Central Ethiopia. *Land* **2022**, *11*, 500. [CrossRef]
36. Sahle, M.; Saito, O.; Fürst, C.; Demissew, S.; Yeshitela, K. Future land use management effects on ecosystem services under different scenarios in the Wabe River catchment of Gurage Mountain chain landscape, Ethiopia. *Sustain. Sci.* **2019**, *14*, 175–190. [CrossRef]
37. Nasir, N.; Selvakumar, R. Influence of land use changes on spatial erosion pattern, a time series analysis using RUSLE and GIS: The cases of Ambuliyar sub-basin, India. *Acta Geophys.* **2018**, *66*, 1121–1130. [CrossRef]
38. Alemu, B.; Garedew, E.; Eshetu, Z.; Kassa, H. Land use and land cover changes and associated driving forces in north western lowlands of Ethiopia. *Int. Res. J. Agric. Sci. Soil Sci.* **2015**, *5*, 28–44.
39. Dibaba, W.T.; Demissie, T.A.; Miegel, K. Drivers and implications of land use/land cover dynamics in Finchaa catchment, northwestern Ethiopia. *Land* **2020**, *9*, 113. [CrossRef]

40. Hailu, A.; Mammo, S.; Kidane, M. Dynamics of land use, land cover change trend and its drivers in Jimma Geneti District, Western Ethiopia. *Land Use Policy* **2020**, *99*, 105011. [CrossRef]
41. Shawul, A.A.; Chakma, S. Spatiotemporal detection of land use/land cover change in the large basin using integrated approaches of remote sensing and GIS in the Upper Awash basin, Ethiopia. *Environ. Earth Sci.* **2019**, *78*, 141. [CrossRef]
42. Ministry of Water, Irrigation and Energy of Ethiopia (MoWIE). Available online: www.mowe.gov.et (accessed on 15 January 2021).
43. Betru, T.; Tolera, M.; Sahle, K.; Kassa, H. Trends and drivers of land use/land cover change in Western Ethiopia. *Appl. Geogr.* **2019**, *104*, 83–93. [CrossRef]
44. Jemberie, M.; Gebrie, T.; Gebremariam, B. Evaluation of land use land cover change on stream flow: A case study of Dedissa Sub Basin, Abay Basin, South Western Ethiopia. *Int. J. Innov. Eng. Res. Technol.* **2016**, *3*, 2394–3696.
45. Fasika, A.; Motuma, T.; Gizaw, T. Land use land cover change trend and its drivers in Somodo watershed, south-western Ethiopia. *Afr. J. Agric. Res.* **2019**, *14*, 102–117. [CrossRef]
46. Kindu, M.; Schneider, T.; Teketay, D.; Knoke, T. Land use/land cover change analysis using object-based classification approach in Munessa-Shashemene landscape of the Ethiopian highlands. *Remote Sens.* **2013**, *5*, 2411–2435. [CrossRef]
47. Abijith, D.; Saravanan, S. Assessment of land use and land cover change detection and prediction using remote sensing and CA Markov in the northern coastal districts of Tamil Nadu, India. *Environ. Sci. Pollut. Res.* **2021**, 1–13. [CrossRef]
48. Patil, M.B.; Desai, C.G.; Umrikar, B.N. Image classification tool for land use/land cover analysis: A comparative study of maximum likelihood and minimum distance method. *Int. J. Geol. Earth Environ. Sci.* **2012**, *2*, 189–196.
49. Soomro, A.G.; Babar, M.M.; Arshad, M.; Memon, A.; Naeem, B.; Ashraf, A. Spatiotemporal variability in spate irrigation systems in Khirthar National Range, Sindh, Pakistan (case study). *Acta Geophys.* **2020**, *68*, 219–228. [CrossRef]
50. Balha, A.; Mallick, J.; Pandey, S.; Gupta, S.; Singh, C.K. A comparative analysis of different pixel and object-based classification algorithms using multi-source high spatial resolution satellite data for LULC mapping. *Earth Sci. Inform.* **2021**, *14*, 2231–2247. [CrossRef]
51. Rwanga, S.S.; Ndambuki, J.M. Accuracy assessment of land use/land cover classification using remote sensing and GIS. *Int. J. Geosci.* **2017**, *8*, 611. [CrossRef]
52. Aliani, H.; Malmir, M.; Sourodi, M.; Kafaky, S.B. Change detection and prediction of urban land use changes by CA–Markov model (case study: Talesh County). *Environ. Earth Sci.* **2019**, *78*, 546. [CrossRef]
53. Gidey, E.; Dikinya, O.; Sebego, R.; Segosebe, E.; Zenebe, A. Modeling the Spatio-temporal dynamics and evolution of land use and land cover (1984–2015) using remote sensing and GIS in Raya, Northern Ethiopia. *Modeling Earth Syst. Environ.* **2017**, *3*, 1285–1301. [CrossRef]
54. Kumar, K.S.; Bhaskar, P.U.; Padmakumari, K. Application of land change modeler for prediction of future land use land cover: A case study of Vijayawada City. *Int. J. Adv. Technol. Eng. Sci.* **2015**, *3*, 773–783.
55. Aryaguna, P.A.; Saputra, A.N. Land change modeler for predicting land cover change in Banjarmasin City, South Borneo (2014–2022). *IOP Conf. Ser. Earth Environ. Sci.* **2020**, *500*, 012002. [CrossRef]
56. Mishra, V.N.; Rai, P.K.; Prasad, R.; Punia, M.; Nistor, M.M. Prediction of spatio-temporal land use/land cover dynamics in rapidly developing Varanasi district of Uttar Pradesh, India, using geospatial approach: A comparison of hybrid models. *Appl. Geomat.* **2018**, *10*, 257–276. [CrossRef]
57. Hasan, S.; Shi, W.; Zhu, X.; Abbas, S.; Khan, H.U.A. Future simulation of land use changes in rapidly urbanizing South China based on land change modeler and remote sensing data. *Sustainability* **2020**, *12*, 4350. [CrossRef]
58. Khoshnood Motlagh, S.; Sadoddin, A.; Haghnegahdar, A.; Razavi, S.; Salmanmahiny, A.; Ghorbani, K. Analysis and prediction of land cover changes using the land change modeler (LCM) in a semiarid river basin, Iran. *Land Degrad. Dev.* **2021**, *32*, 3092–3105. [CrossRef]
59. Rumelhart, D.E.; Hinton, G.E.; Williams, R.J. Learning internal representations by error propagation. In *Parallel Distributed Processing*; Rumelhart, D.E., McClelland, J.L., Eds.; MIT Press: Cambridge, MA, USA, 1986; pp. 318–362.
60. Mishra, V.N.; Rai, P.K.; Mohan, K. Prediction of land use changes based on land change modeler (LCM) using remote sensing: A case study of Muzaffarpur (Bihar), India. *J. Geogr. Inst. "Jovan Cvijic" SASA* **2014**, *64*, 111–127. [CrossRef]
61. Clark Labs. *TerrSet (18.3) [Software]*; Clark University: Worcester, MA, USA, 2017.
62. Shade, C.; Kremer, P. Predicting land use changes in Philadelphia following green infrastructure policies. *Land* **2019**, *8*, 28. [CrossRef]
63. Ibrahim, M.M.; Duker, A.; Conrad, C.; Thiel, M.; Shaba Ahmad, H. Analysis of settlement expansion and urban growth modelling using geoinformation for assessing potential impacts of urbanization on climate in Abuja City, Nigeria. *Remote Sens.* **2016**, *8*, 220. [CrossRef]
64. Wang, J.; Maduako, I.N. Spatio-temporal urban growth dynamics of Lagos Metropolitan Region of Nigeria based on Hybrid methods for LULC modeling and prediction. *Eur. J. Remote Sens.* **2018**, *51*, 251–265. [CrossRef]
65. Wang, W.; Zhang, C.; Allen, J.M.; Li, W.; Boyer, M.A.; Segerson, K.; Silander, J.A. Analysis and prediction of land use changes related to invasive species and major driving forces in the state of Connecticut. *Land* **2016**, *5*, 25. [CrossRef]
66. Cramer, H. *Mathematical Methods of Statistics (PMS-9)*; Princeton University Press: Princeton, NJ, USA, 2016; Volume 9.
67. Beh, E.J. Theory & Methods: Partitioning Pearson's Chi-squared Statistic for Singly Ordered Two-way Contingency Tables. *Aust. New Zealand J. Stat.* **2001**, *43*, 327–333.
68. Eastman, J.R. *IDRISI Taiga Guide to GIS and Image Processing*; Clark Labs Clark University: Worcester, MA, USA, 2009.

69. Gaur, S.; Mittal, A.; Bandyopadhyay, A.; Holman, I.; Singh, R. Spatio-temporal analysis of land use and land cover change: A systematic model inter-comparison driven by integrated modelling techniques. *Int. J. Remote Sens.* **2020**, *41*, 9229–9255. [CrossRef]
70. Benavidez-Silva, C.; Jensen, M.; Pliscoff, P. Future Scenarios for Land Use in Chile: Identifying Drivers of Change and Impacts over Protected Area System. *Land* **2021**, *10*, 408. [CrossRef]
71. Vu, T.T.; Shen, Y. Land-Use and Land-Cover Changes in Dong Trieu District, Vietnam, during Past Two Decades and Their Driving Forces. *Land* **2021**, *10*, 798. [CrossRef]
72. Kafi, K.M.; Shafri, H.Z.M.; Shariff, A.B.M. An analysis of LULC change detection using remotely sensed data; A Case study of Bauchi City. *IOP Conf. Ser. Earth Environ. Sci.* **2014**, *20*, 012056. [CrossRef]
73. Vivekananda, G.N.; Swathi, R.; Sujith, A.V.L.N. Multi-temporal image analysis for LULC classification and change detection. *Eur. J. Remote Sens.* **2021**, *54*, 189–199. [CrossRef]
74. Hishe, S.; Bewket, W.; Nyssen, J.; Lyimo, J. Analysing past land use land cover change and CA-Markov-based future modelling in the Middle Suluh Valley, Northern Ethiopia. *Geocarto Int.* **2020**, *35*, 225–255. [CrossRef]
75. Tsegaye, D.; Moe, S.R.; Vedeld, P.; Aynekulu, E. Land-use/cover dynamics in Northern Afar rangelands, Ethiopia. *Agric. Ecosyst. Environ.* **2010**, *139*, 174–180. [CrossRef]
76. Minale, A.S.; Rao, K.K. Impacts of land cover/use dynamics of Gilgel Abbay catchment of Lake Tana on climate variability, Northwestern Ethiopia. *Appl. Geomat.* **2012**, *4*, 155–162. [CrossRef]
77. Müller-Mahn, D.; Gebreyes, M. Controversial connections: The water-energy-food nexus in the Blue Nile basin of Ethiopia. *Land* **2019**, *8*, 135. [CrossRef]
78. Gebrehiwot, S.G.; Bewket, W.; Gardenas, A.I.; Bishop, K. Forest cover change over four decades in the Blue Nile Basin, Ethiopia: Comparison of three watersheds. *Reg. Environ. Change* **2014**, *14*, 253–266. [CrossRef]
79. Meshesha, D.T.; Tsunekawa, A.; Tsubo, M.; Ali, S.A.; Haregeweyn, N. Land-use change and its socio-environmental impact in Eastern Ethiopia's highland. *Reg. Environ. Change* **2014**, *14*, 757–768. [CrossRef]
80. Regasa, M.; Nones, M. Land Use Land Cover Changes in the Fincha Basin, Ethiopia. In Proceedings of the 39th IAHR World Congress, Granada, Spain, 19–24 June 2022; Volume 19, p. 24.
81. Berisso, T. Deforestation and environmental degradation in Ethiopia: The case of Jam Jam Province. *Northeast Afr. Stud.* **1995**, *2*, 139–155. [CrossRef]
82. Dessie, G.; Kleman, J. Pattern and magnitude of deforestation in the south central rift valley region of Ethiopia. *Mt. Res. Dev.* **2007**, *27*, 162–168. [CrossRef]
83. Federal Democratic Republic of Ethiopia-FDRE. *Constitution of the Federal Democratic Republic of Ethiopia*; National Legislative Bodies/National Authorities: Addis Ababa, Ethiopia, 1994; p. 50.
84. Watson, C. Direct Consumptive Use Valuation of the Ecosystem Goods and Services in the Bale Mountains Eco-Region, Ethiopia. Doctoral Dissertation, Centre of Environmental Policy, Faculty of Natural Sciences, Imperial College London, London, UK, 2007.
85. Dejene, T.; Lemenih, M.; Bongers, F. Manage or convert Boswellia woodlands? Can frankincense production payoff? *J. Arid Environ.* **2013**, *89*, 77–83. [CrossRef]
86. Tolessa, T.; Kidane, M.; Bezie, A. Assessment of the linkages between ecosystem service provision and land use/land cover change in Fincha watershed, North-Western Ethiopia. *Heliyon* **2021**, *7*, e07673. [CrossRef] [PubMed]
87. Tessema, I.; Simane, B. Vulnerability analysis of smallholder farmers to climate variability and change: An agro-ecological system-based approach in the Fincha'a sub-basin of the upper Blue Nile Basin of Ethiopia. *Ecol. Processes* **2019**, *8*, 5. [CrossRef]
88. Tefera, B.; Sterk, G. Hydropower-induced land use change in Fincha'a watershed, western Ethiopia: Analysis and impacts. *Mt. Res. Dev.* **2008**, *28*, 72–80. [CrossRef]
89. Mariye, M.; Maryo, M.; Li, J. The study of land use and land cover (LULC) dynamics and the perception of local people in Aykoleba, northern Ethiopia. *J. Indian Soc. Remote Sens.* **2022**, *50*, 775–789. [CrossRef]
90. Senbeta, F. Community perception of land use/land cover change and its impacts on biodiversity and ecosystem services in northwestern Ethiopia. *J. Sustain. Dev. Afr.* **2018**, *20*, 108–126.